J. Fluid Mech. (1988), *vol.* 190, *pp.* 343–356
Printed in Great Britain

Incoherent turbulence structure in the near wake of a normal plate

By M. KIYA AND M. MATSUMURA
Department of Mechanical Engineering, Hokkaido University, Sapporo, 060 Japan

(Received 6 May 1987 and in revised form 24 August 1987)

In this paper experimentally studied characteristics of various frequency components of incoherent velocity fluctuations in the near wake behind a thin normal plate immersed in a uniform flow are described. Measurements were made at a position 8 plate heights downstream of the plate where the wake had a marked periodicity, so that coherent vortices shed from the plate are expected to have a small dispersion in streamwise spacing, transverse location, strength and shape. Shearing stress associated with the incoherent fluctuations is mainly contributed by components with frequencies around half of the vortex-shedding frequency f_s on one side of the wake. The $\frac{1}{2}f_s$ frequency component appears to be caused by the spanwise locations of ribs, which are connected to the coherent vortices, being different from vortex to vortex. A probable spanwise arrangement of the ribs is suggested.

1. Introduction

Turbulence structure in plane wakes of cylindrical bodies has recently been studied by phase-averaging techniques; see, for example, the works of Cantwell and Coles (1983), Hayakawa & Hussain (1985, 1986), Kiya & Matsumura (1985), Perry & Steiner (1987), Steiner & Perry (1987), Antonia *et al.* (1987). In these studies an instantaneous quantity S in the wake is decomposed into a time-mean or global component $\bar{S}$, a phase-averaged or coherent component $\tilde{s}$, and a random or incoherent component s':

$$S = \bar{S} + \tilde{s} + s'$$

in the triple decomposition scheme (Reynolds & Hussain 1972). Also, let

$$s = \tilde{s} + s'.$$

A coherent structure means a structure associated with the phase-averaged components while an incoherent structure is a structure corresponding to the random components.

Those studies mentioned above have described the coherent structures in a streamwise plane normal to the spanwise direction, although their three-dimensional aspects are not clarified yet. Entrainment and mixing of outer irrotational fluid, production of the incoherent turbulence and its transport are interpreted in terms of the flow induced by the coherent structures. It is now believed that, in free turbulent shear flows, the incoherent turbulence is produced by the stretching of longitudinal vortices (or ribs) aligned along the diverging separatrix of a saddle between two consecutive coherent structures (Cantwell & Coles 1983; Hussain 1986). In the terminology of Hussain (1986), the ribs are a coherent substructure; they produce random components because their spanwise positions are expected to be rather

randomly distributed (from rib to rib) between two consecutive coherent structures.

On the other hand, the dynamical significance of the random components in the wakes can be demonstrated by the fact that they contribute to most of the global Reynolds stresses (Hussain 1981; Cantwell & Coles 1983; Perry & Steiner 1987; Steiner & Perry 1987). The incoherent components also play an essential role in small-scale mixing processes, which are of vital importance in combustion and in chemical reactions. However, many aspects of the incoherent components remain unknown.

The purpose of this paper is to study experimentally characteristics of various frequency components of the random velocity fluctuations in the near wake behind a thin normal plate immersed in a uniform flow. We expect such a frequency analysis to yield further information on the incoherent turbulence. Measurements were made at a position 8 plate heights downstream of the front face of the plate where the wake had a marked periodicity, so that vortices shed from the plate are expected to have a small dispersion in streamwise spacing, transverse location, strength and shape. The normal plate was used in order to have a straight line of flow separation along the edges, so that the initial spanwise waviness of the shed vortices is expected to be smaller than that of the vortices behind a cylindrical body with a smooth change of surface curvature, e.g. a circular cylinder.

The most important findings of this study are that the random shearing stress is mainly contributed by components with frequencies of around half of the vortex-shedding frequency on a side of the wake, and that this is caused by the spanwise locations of the ribs being different from saddle to saddle. A plausible spanwise arrangement of the ribs is presented.

2. Experimental apparatus

Experiments were performed in an open-return wind tunnel with a 0.30 m × 0.30 m square and 1.01 m long working section. The air was sucked through a filter into a calming chamber, then flowed into the working section through a 9:1 contraction after passing two-stage screens in the calming chamber. The sidewalls of the tunnel had narrow slits for traversing hot-wire probes; the slits were tightly sealed during measurements.

The tunnel allows main-flow velocities up to 21 m/s. The longitudinal turbulence intensity was approximately 0.2% at a main-flow velocity $U_\infty = 16.4$ m/s, which is the velocity used in the present experiment. The main-flow velocity and the turbulence intensity were uniform to within $\pm 0.005 U_\infty$ and $\pm 0.001 U_\infty$, respectively, in a normal plane 0.30 m downstream of the entrance of the working section; the front face of a wake-generating normal plate was located in this plane.

The plate, of height $h = 2.0$ cm, was manufactured from smooth brass sheet 0.43 cm in thickness. The edges of the plate were bevelled to an angle of 30° towards the rear side. The plate was set normal to the main flow, spanning the central part of the working section. No end plate was employed. Thus the aspect ratio of the plate was 15, the tunnel-wall blockage being 6.7%.

Velocity fluctuations in the wake were measured by X-wire probes operated by constant-temperature hot-wire anemometers; the hot wires were inclined by $\pm 45°$ towards the streamwise direction. The diameter of the wires was 0.005 mm and their working length was about 1 mm. The overheat ratio was set at 1.5. A square-wave test showed that the maximum frequency of response was greater than 10 kHz.

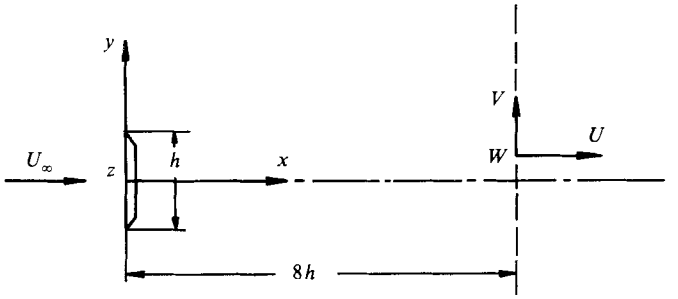

FIGURE 1. Configuration of flow and definition of symbols. Measurements were made at a position 8 plate heights downstream of a plate.

Voltage signals from the anemometers were recorded on to four channels of an analogue tape recorder and later sampled via a 12-bit A/D converter with a sampling rate of 20 kHz. The digital data were analysed by a HITAC M-680H computer installed at the Hokkaido University Computing Centre.

Measurements were made in a normal plane $8h$ downstream of the front face of the plate. The Reynolds number based on the plate height was 23000. The vortex-shedding frequency f_s on one side of the wake was 120 Hz, so that the Strouhal number $f_s h/U_\infty$ is 0.146. The sampling rate of 20 kHz is approximately 170 times the vortex-shedding frequency.

3. Eduction of structures and phase averaging

As shown in figure 1, the Cartesian coordinates x, y, z are defined in such a way that the x-axis is in the streamwise direction, the y-axis is vertically upwards along the front face of the plate, and the z-axis is normal to the x- and y-axes so as to form a right-handed system; the origin is located at the centre of the front face in the midspan plane. The instantaneous velocity components in the x-, y- and z-directions are respectively denoted by U, V, W; the instantaneous vorticity component in the z-direction is Ω.

Coherent structures are vortical structures, so that it would be most appropriate to educe the former on the basis of an instantaneous vorticity distribution (Hussain 1986). This is particularly true for fully developed turbulent shear flows, where coherent structures appear randomly in space and time. However, in an x-range of the wake up to several heights downstream of the plate, coherent structures are large vortices shed with a marked periodicity from the plate; these are 'rolls' in the terminology of Hussain (1986). The coherent structures produce large fluctuations in v ($= \tilde{v}+v'$), especially at positions on the time-mean centre of the wake; an example is shown in figure 2(a). In that x-range we expect a small dispersion in the coherent structures, i.e. a small dispersion in spanwise spacing, transverse location, strength and shape. Thus the coherent structures can be educed by a phase-averaging scheme in which a conditioning signal is a bandpass-filtered time history of v, say v_f, the central frequency of the (digital) bandpass filter being the average vortex-shedding frequency f_s. Figure 2(b) shows the bandpass-filtered signal of v in figure 2(a).

In the present experiment phase-averaged signals were measured at various y-positions on a normal straight line (from now on denoted by the line of measurement), $(x, y, z)/h = (8.0, y/h, 0)$ while the conditioning signal v_f was obtained at a nearby position $(x, y, z)/h = (8.0, 0, 0.25)$. The phase-averaging was conducted

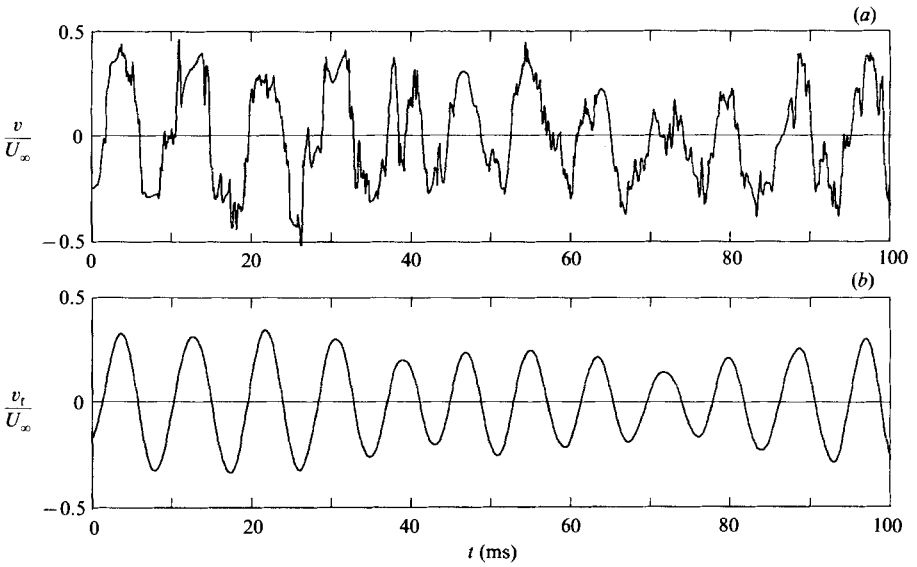

FIGURE 2. (*a*) An example of cross-stream velocity fluctuation v measured at a position $(x, y, z)/h = (8.0, 0, 0.25)$ on the time-mean centre of the wake; and (*b*) its bandpass-filtered waveform v_f, which is a conditioning signal for phase averaging. The origin of time is arbitrary, but the same for both (*a*) and (*b*).

for all periods of the conditioning signal. This is consistent with the foregoing assumption that the dispersion in the coherent structures is small.

The phase averaging was initiated by detecting two consecutive instants t_1 and t_2 ($> t_1$), when the conditioning signal v_f respectively satisfied the conditions $v_f = 0$, $dv_f/dt > 0$ and $v_f = 0$, $dv_f/dt < 0$. The interval $t_2 - t_1$ had an average value $T_s (= 1/f_s)$, which is the average vortex-shedding period, and a standard deviation $0.17T_s$. Each interval $t_2 - t_1$ was aligned relative to T_s (that is, $t_2 - t_1$ was made equal to T_s), and then the phase averaging was done at times $t_1 + (nT_s/120)$, where $n = 0, 1, \ldots, 120$. The number N of the phase-averaged realizations was 1200; this means that the signals over a period of 10 s were used since T_s was equal to 1/120 s. This value of N was large enough to yield stable phase-averaged patterns to be presented in §4.

4. Results

In §§4.1 and 4.2 we present a few typical results in order to show that they are consistent with the previous studies (Cantwell & Coles 1983; Hayakawa & Hussain 1985, 1986; Perry & Steiner 1987; Steiner & Perry 1987). Fairly good two-dimensionality of the time-mean quantities in the wake was realized. This was demonstrated partly by the root-mean-square velocities $(\overline{u^2})^{\frac{1}{2}}$ and $(\overline{v^2})^{\frac{1}{2}}$ being uniform in the spanwise z-direction to within $\pm 3.5\%$ of their average values, and partly by the time-mean spanwise velocity $\overline{W}$ being only of the order $0.02U_\infty$ in the wake.

4.1 *Time-mean velocities and Reynolds stresses*

The time-mean streamwise velocity $\bar{U}$ and the Reynolds stresses are shown in figure 3. The time-mean crossflow velocity $\bar{V}$ (not shown here) was at most of the order of $0.02U_\infty$. Figure 3 indicates that the normal stresses $\overline{u^2}$ ($= \tilde{u}^2 + \overline{u'^2}$), $\overline{w^2}$ ($= \tilde{w}^2 + \overline{w'^2}$) and the shearing stress $\overline{uv}$ ($= \tilde{u}\tilde{v} + \overline{u'v'}$) are produced mostly by the random components,

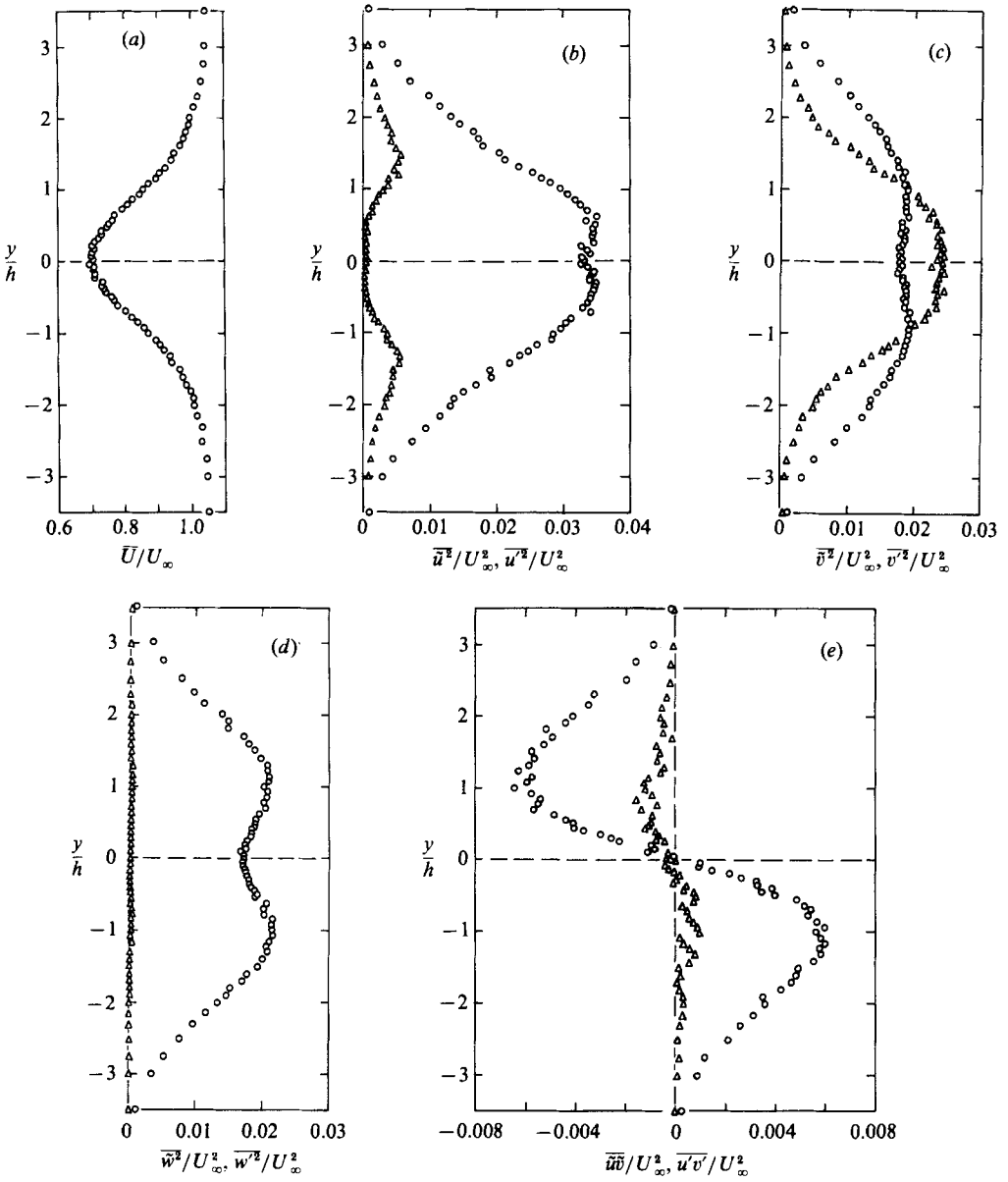

FIGURE 3. Profiles of (*a*) time-mean streamwise velocity $\overline{U}$; normal stresses (*b*) $\overline{\tilde{u}^2}/U_\infty^2$ (△), $\overline{u'^2}/U_\infty^2$ (○), (*c*) $\overline{\tilde{v}^2}/U_\infty^2$ (△), $\overline{v'^2}/U_\infty^2$ (○), (*d*) $\overline{\tilde{w}^2}/U_\infty^2$ (△), $\overline{w'^2}/U_\infty^2$ (○); and (*e*) shearing stresses $\overline{\tilde{u}\tilde{v}}/U_\infty^2$ (△), $\overline{u'v'}/U_\infty^2$ (□) measured at $8h$ downstream of a normal plate.

whereas the crossflow normal stress $\overline{v^2}$ $(=\overline{\tilde{v}^2}+\overline{v'^2})$ is contributed equally to by the coherent component and the random component. This demonstrates the dynamical significance of the random components, being consistent with the results of Cantwell & Coles, Perry & Steiner and Steiner & Perry.

4.2. *Coherent vorticity, incoherent energy and shearing stress*

The coherent vorticity $\tilde{\omega} = \partial(\bar{V}+\tilde{v})/\partial x - \partial(\bar{U}+\tilde{u})/\partial y$ is shown in figure 4. The differentiation with respect to the streamwise coordinate x was evaluated by

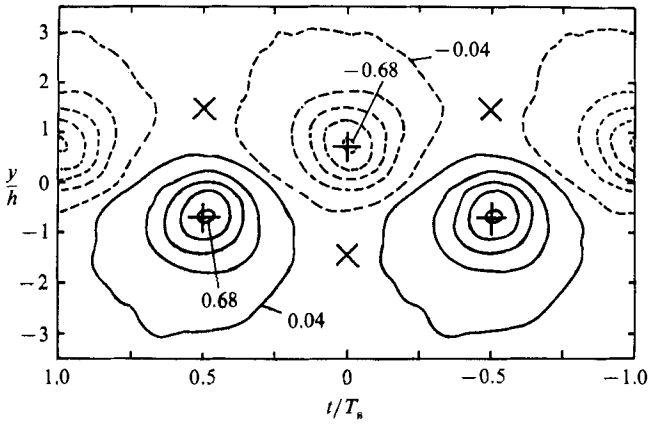

FIGURE 4. Contours for coherent spanwise vorticity $\tilde{\omega}h/U_\infty$ (contour interval 0.16): ×, saddles; +, centres.

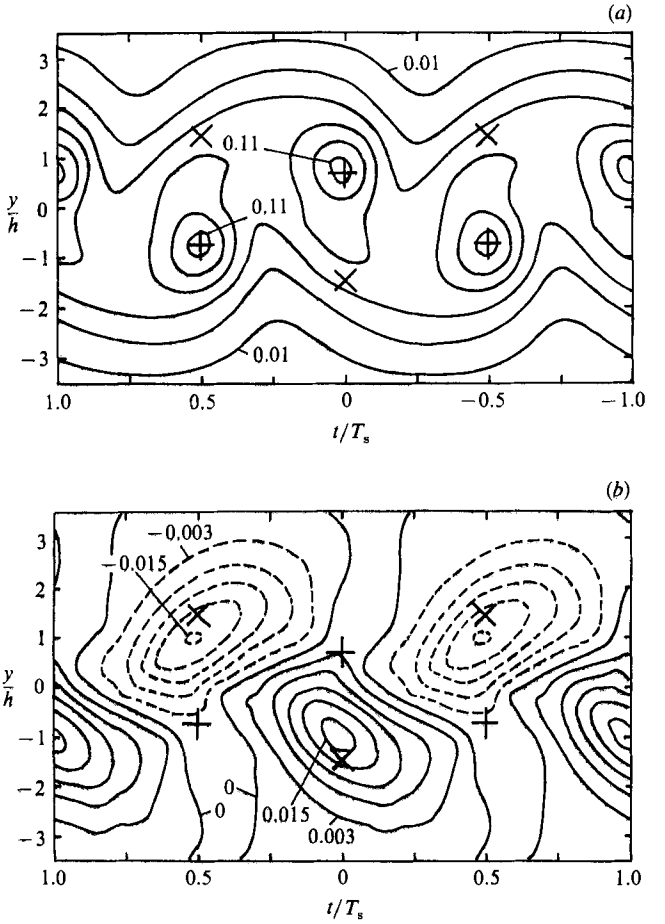

FIGURE 5. Contours for (*a*) incoherent energy $\langle q'^2 \rangle U_\infty^2$ (contour interval 0.02) and (*b*) incoherent shearing stress $\langle \overline{u'v'} \rangle / U_\infty^2$ (contour interval 0.003).

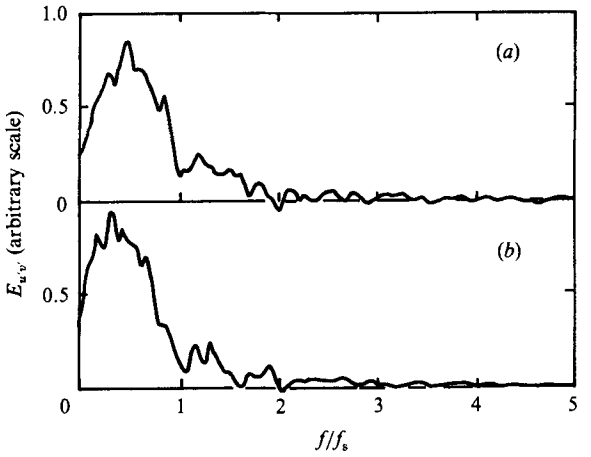

FIGURE 6. Real part of cross-spectrum of incoherent fluctuations u', v' measured at $8h$ downstream of a normal plate: (*a*) $y/h = -0.7$; (*b*) -1.4.

assuming Taylor's hypothesis $\mathrm{d}x = -U_c \mathrm{d}t$, U_c being the convection velocity of the centre of the coherent structure. A method of determining U_c will be described in the next paragraph. The velocity-vector field $(\bar{U} + \tilde{u} - U_c, \bar{V} + \tilde{V})$ (not shown here) had saddles and centres whose locations are indicated in figure 4.

The convection velocity U_c was obtained in terms of the space–time (y, t) distribution of the streamwise velocity component $\bar{U} + \tilde{u}$. Tentatively assuming a centre of the coherent structure at a position $(y^{(1)}, t^{(1)})$ in the space–time domain and then obtaining the first approximation $U_c^{(1)}$ to the convection velocity, we constructed a vorticity distribution such as shown in figure 4. This distribution determined the second approximations of the centre position $(Y^{(2)}, t^{(2)})$ and the convection velocity $U_c^{(2)}$, the latter being the value of $\bar{U} + \tilde{u}$ at the centre. Convergence was obtained after a few iterations; the y-coordinate of the centre was at $y/h = \pm 0.74$ and the convection velocity was equal to $U_c/U_\infty = 0.85$.

Space–time distributions of the random energy $\langle q'^2 \rangle (= \langle u'^2 \rangle + \langle v'^2 \rangle + \langle w'^2 \rangle)$ and shearing stress $\langle u'v' \rangle$ are presented in figure 5. We shall call the product $\langle u'v' \rangle$ a shearing stress; from now on the product $u'v'$ will also be termed a shearing stress. Figure 5 shows the well-documented feature that the energy attains a maximum near the centre of the coherent structures whereas the shearing stress $\langle u'v' \rangle$ attains a maximum near the saddles (Hussain 1981; Cantwell & Coles 1983).

4.3. *Frequency analysis of random components*

In order to examine the dynamical role of various frequency components of the random fluctuations, the real part of the cross-spectrum of u' and v', say $E_{u'v'}$, and the power spectra of all the velocity fluctuations $E_{u'}$, $E_{v'}$, $E_{w'}$ are shown in figures 6 and 7. The cross-spectrum demonstrates that most of the shearing stress $\overline{u'v'}$ is produced by low-frequency components with $f < f_s$, f being the frequency; in particular, the most significant contribution appears to come from frequency components around $f = \frac{1}{2}f_s$. On the other hand, those low-frequency components contribute to only about a half of the energy $\overline{u'^2}$, and to a much smaller fraction of the energy $\overline{v'^2}$ and $\overline{w'^2}$.

More detailed information on the dynamical role of each frequency component can be obtained from the space–time distributions of the energy and shearing stress

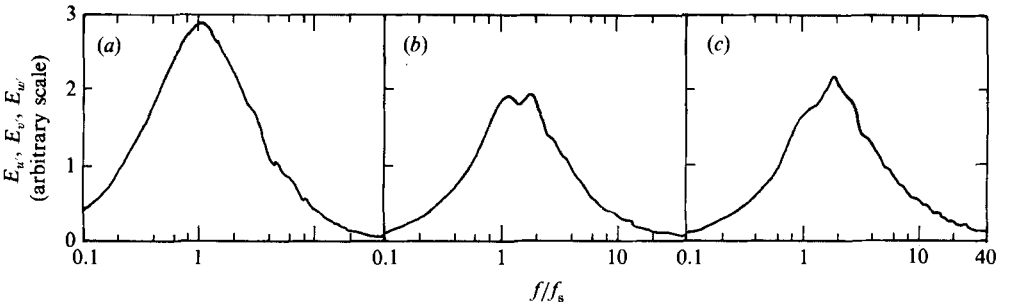

FIGURE 7. Power spectra of incoherent fluctuations u', v', w' measured at $y/h = 0.7$ and at $8h$ downstream of a normal plate: (*a*) fE'_u; (*b*) fE'_v; (*c*) fE'_w.

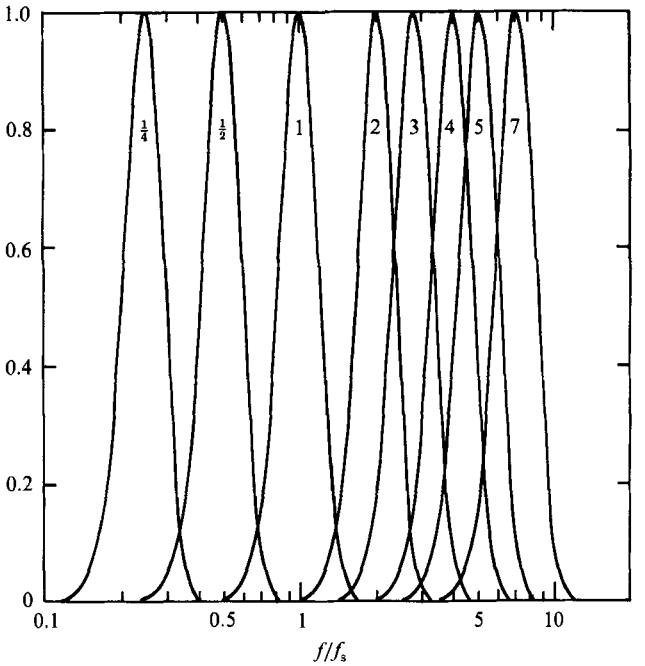

FIGURE 8. The use of bandpass filters to extract frequency components of incoherent fluctuations. Inserted numbers show values of a (see text). The vertical axis is the ratio of output to input signal.

associated with that component. Several typical frequency components were obtained by passing the random fluctuations through digital bandpass filters. This is shown in figure 8. Each frequency component of the random fluctuations will be denoted by a suffix a, which is the central frequency f_c of the corresponding bandpass filter divided by the vortex-shedding frequency f_s, i.e. $a = f_c/f_s$; the corresponding velocity components are represented by u'_a, v'_a, w'_a. Components were obtained for $a = \frac{1}{4}$, $\frac{1}{2}$, 1, 2, 3, 4, 5 and 7.

The energy $\langle q'^2_a \rangle$ and the shearing stress $\langle u'_a v'_a \rangle$ are shown in figures 9 and 10 for $a = \frac{1}{2}$, 1, 2 and 3. Corresponding patterns for $a = 4$, 5 and 7 are not presented because they are similar to those for $a = 3$. The lowest-frequency components $\langle q'^2_{\frac{1}{4}} \rangle$ and $\langle u'_{\frac{1}{4}} v'_{\frac{1}{4}} \rangle$ were found to be uncorrelated to the phases of the conditioning signal v_f. The energy for $a \geqslant 2$ attains a maximum at the centre of the coherent structure,

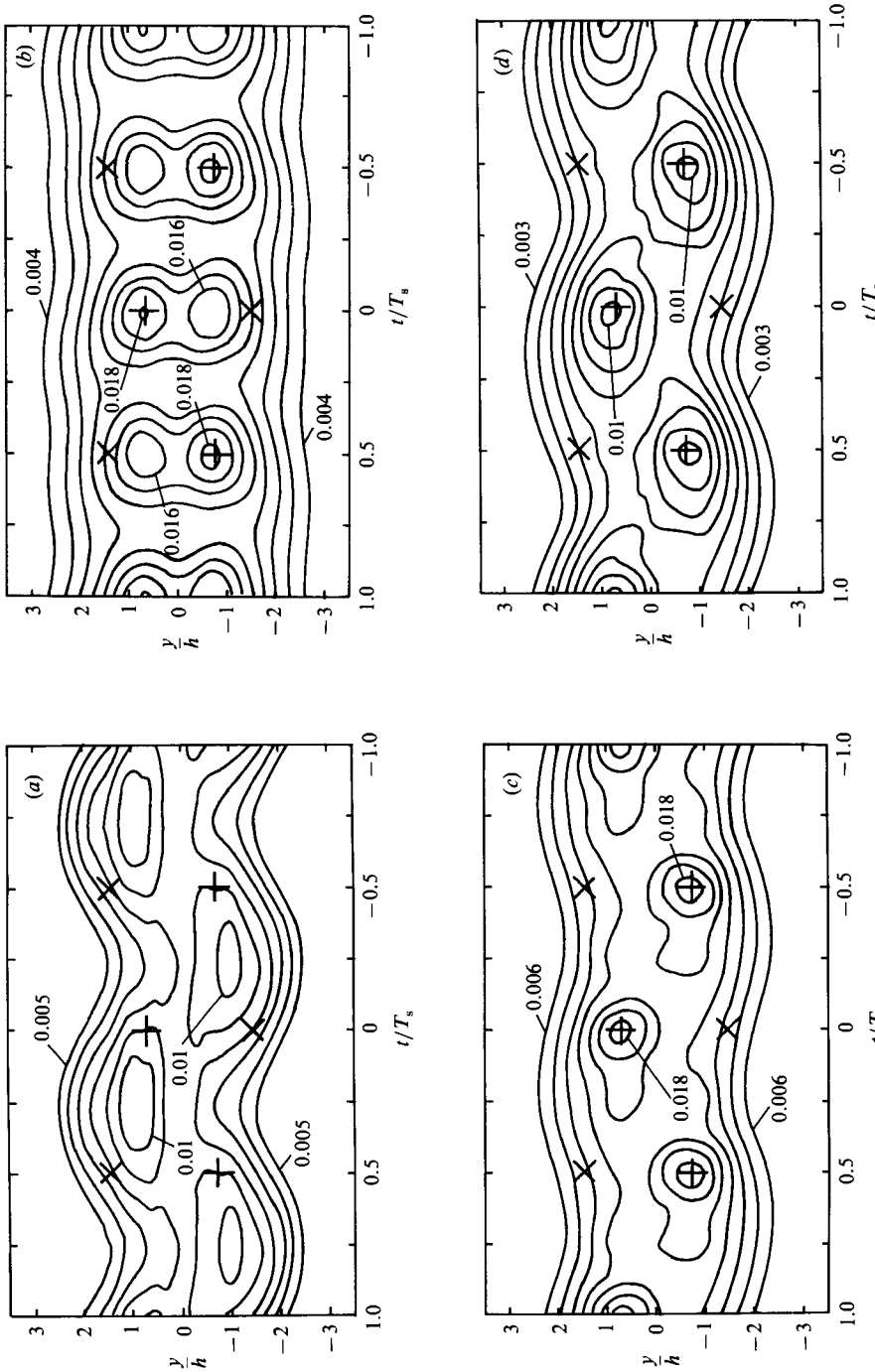

FIGURE 9. Contours for incoherent energy $\langle q_a'^2 \rangle / U_\infty^2$: (*a*) $a = \frac{1}{2}$ (contour interval 0.001); (*b*) $a = 1$ (contour interval 0.002); (*c*) $a = 2$ (contour interval 0.002); (*d*) $a = 3$ (contour interval 0.001).

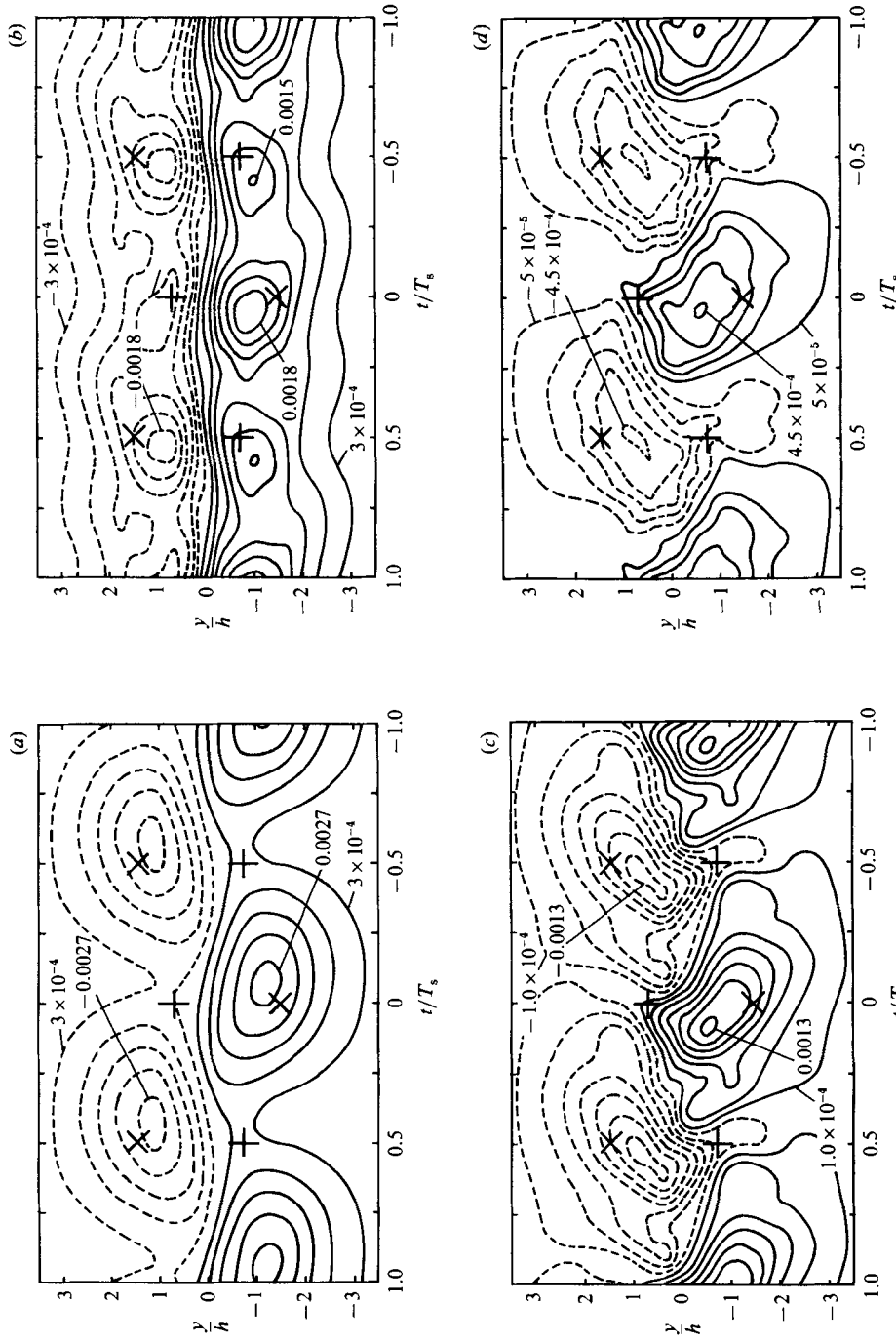

FIGURE 10. Contours for incoherent shearing stress $\langle u_a' v_a' \rangle / U_\infty^2$: (*a*) $a = \frac{1}{2}$ (contour interval 6.0×10^{-4}); (*b*) $a = 1$ (contour interval 3.0×10^{-4}); (*c*) $a = 2$ (contour interval 2.0×10^{-4}); (*d*) $a = 3$ (contour interval 1.0×10^{-4}).

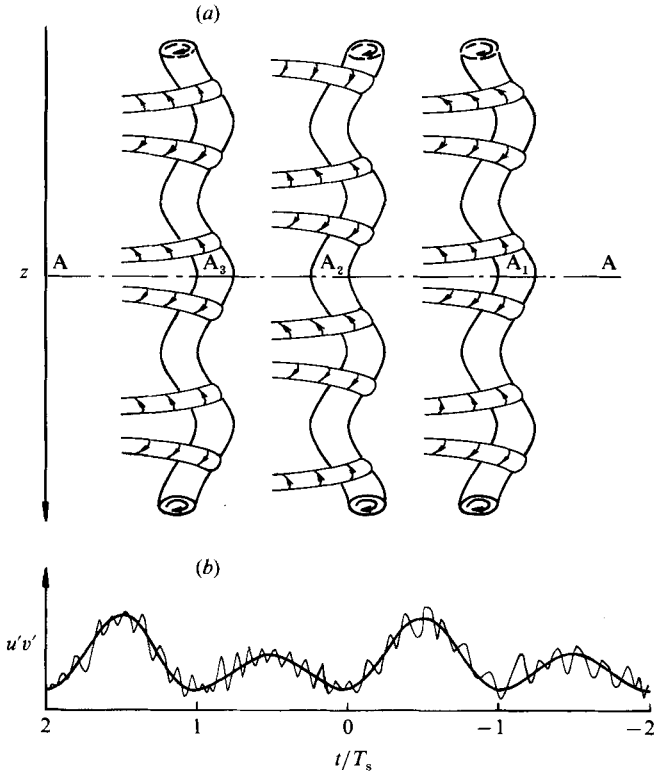

FIGURE 11. Sketches of (*a*) plasusible arrangement of ribs and rolls on one side of the wake, and (*b*) corresponding waveform of $u'v'$ measured on a line AA (thin solid line) and its short-time-averaged waveform (thick solid line). Flow is from left to right. The sketch of the waveform is shown to visualize the generation of the subharmonic component. It was difficult to perceive the subharmonic component in the actual waveform.

whereas $\langle q_{\frac{3}{2}}'^2 \rangle$ attains a maximum between a centre and a succeeding saddle; the energy $\langle q_1'^2 \rangle$ ha a symmetrical double-peak distribution. Thus the total random energy $\langle q'^2 \rangle$ with a peak only at the centre is mainly caused by the frequency components with $f \geqslant 2f_s$.

It should be noted that the shearing-stress component $\langle u_{\frac{1}{2}}' v_{\frac{1}{2}}' \rangle$ attains a peak near the saddles and that this component makes the greatest contribution to the global random shearing stress $\overline{u'v'}$. The latter is consistent with figure 6. The next greatest contribution to $\overline{u'v'}$ comes from the fundamental component with the frequency f_s. This can be seen in figure 10 by comparing peak magnitudes of $\langle u_{\frac{1}{2}}' v_{\frac{1}{2}}' \rangle$ and areas enclosed by line corresponding to $\langle u_a' v_a' \rangle / U_\infty^2 = 0.0015$ for $a = \frac{1}{2}$ and 1. The location of a peak value of $\langle u_a' v_a' \rangle$ seems to become more and more remote from the nearby saddle as the value of a increases; a high-frequency component $\langle u_7' v_7' \rangle$ attained no definite peak near the saddles. Accordingly among $\langle u_a' v_a' \rangle$ values the component $\langle u_{\frac{1}{2}}' v_{\frac{1}{2}}' \rangle$ makes the greatest contribution to the random shearing stress $\langle u'v' \rangle$ attaining a peak near the saddles.

5. Discussion and conclusion

The present study has shown that the shearing stress $\overline{uv}$ in a turbulent vortex-street wake is contributed mainly by the component of the random velocity

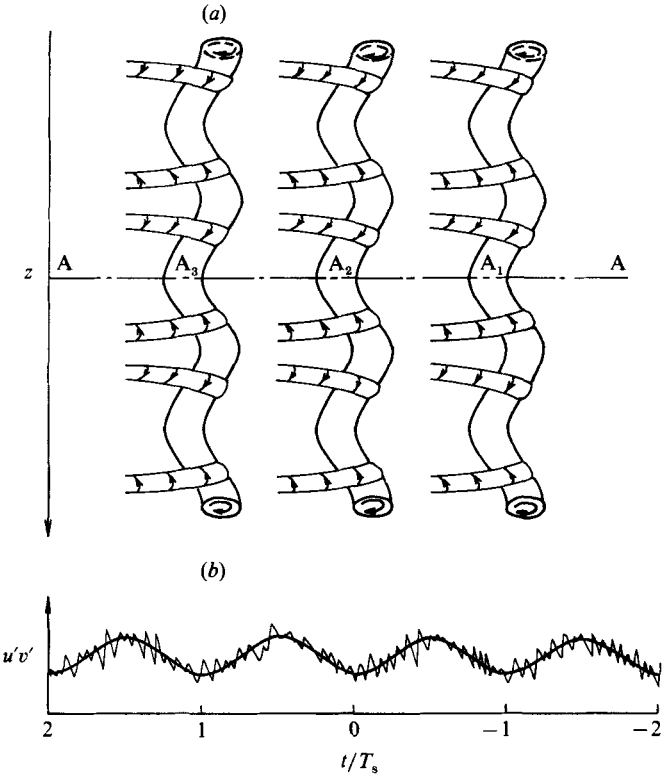

FIGURE 12. Sketches of (*a*) symmetrical arrangement of ribs and rolls on one side of the wake; and (*b*) corresponding waveform of $u'v'$ measured along a line AA (thin solid line) and its short-time-averaged waveform (thick solid line). Flow is from left to right. The sketch of the waveform is shown to visualize the absence of the subharmonic component.

fluctuations with a frequency less than the vortex-shedding frequency f_s; the largest contribution appears to come from the frequency components near $\frac{1}{2}f_s$. Moreover, the random components with the frequency $\frac{1}{2}f_s$ produce the shearing stress $\langle u'_{\frac{1}{2}} v'_{\frac{1}{2}} \rangle$ that attains a maximum near the saddles in the flow field associated with the coherent structures.

It seems difficult to interpret a structure responsible for the components $u'_{\frac{1}{2}}$ and $v'_{\frac{1}{2}}$ in terms of a structure with a larger streamwise extent than that of the coherent structure, because such a large structure cannot be stretched by the smaller coherent structure in such a systematic way for the shearing stress $\langle u'_{\frac{1}{2}} v'_{\frac{1}{2}} \rangle$ to attain a maximum near the saddles. Rather, we prefer to interpret those components $u'_{\frac{1}{2}}$ and $v'_{\frac{1}{2}}$ in terms of different spanwise locations of the ribs between two consecutive rolls. If the ribs are assumed to be arranged as shown in figure 11 (*a*) an X-wire probe fixed on a particular line AA would measure a time history of $u'v'$ depicted schematically in figure 11 (*b*) by a thin solid line. We borrowed the sketch of the ribs connected to a particular roll from Hussain's (1986) 'more realistic picture' (figure 12*d* of his paper). A short-time-averaged signal, which is the thick solid line in figure 11 (*b*), is amplitude-modulated owing to a difference in the magnitude of u' and v' during intervals A_1A_2 and A_2A_3. The short-time-averaged signal has a fundamental frequency $\frac{1}{2}f_s$. It should be emphasized that the pattern of figure 11 (*a*) is the basic one. In reality the spanwise location of the ribs and the corresponding deformation

of the rolls are expected to have random fluctuations around the basic pattern. Such fluctuations can give rise to randomness of the velocity fluctuations u' and v' which nevertheless yield a $u'v'$-waveform with a subharmonic component.†

One could imagine another typical arrangement of the ribs, i.e. the symmetrical one shown in figure 12(*a*). This arrangement, however, yields a short-time-averaged signal of $u'v'$ whose frequency is equal to the vortex-shedding frequency f_s (see figure 12*b*). Accordingly the arrangement of the ribs in figure 11(*a*) is more probable.

Evidence of ribs has been shown for plane mixing layers by flow visualizations (Jimenez, Cogollos & Bernal 1985; Bernal & Roshko 1986; Lasheras, Cho & Maxworthy 1986) and by numerical solutions of the Navier–Stokes equations (Hussain 1986); in flow visualizations of the wake of a circular cylinder and a thin flat plate (Taneda 1986; Meiburg & Lasheras 1987); and in a separated shear layer behind a normal plate by visualization of cavitation bubbles (Katz & O'Hern 1986). As far as the authors are aware, however, no quantitative measurement by hot-wire probes has shown direct evidence of the ribs. Moreover, no experimental or numerical study has disclosed how the ribs are arranged in the spanwise direction from roll to roll. These are future problems to be tackled.

This research was supported by the Grant-in-Aid for Scientific Research A-60420026 from the Ministry of Education, Science and Culture of Japan. We are grateful to Drs M. Hayakawa, O. Mochizuki, Y. Suzuki and H. Tamura for their helpful discussions on the experimental results and to Messrs T. Yamazaki and T. Sampo for their help in constructing the experimental apparatus.

REFERENCES

Antonia, R. A., Browne, L. W. B., Bisset, D. K. & Fulachier, L. 1987 A description of the organized motion in the turbulent far wake of a cylinder at low Reynolds number. *J. Fluid Mech.* **184**, 423–444.

Bernal, L. P. & Roshko, A. 1986 Spanwise vortex structure in plane mixing layers. *J. Fluid Mech.* **170**, 499–525.

Cantwell, B. & Coles, D. 1983 An experimental study of entrainment and transport in the turbulent near wake of a circular cylinder. *J. Fluid Mech.* **136**, 321–374.

Hayakawa, M. & Hussain, A. K. M. F. 1985 Eduction of coherent structures in the turbulent plane wake. In *Proc. 5th Symp. on Turbulent Shear Flows, August 7–9, 1985, Ithaca, New York,* pp. 4.33–4.38. Cornell University.

Hayakawa, M. & Hussain, A. K. M. F. 1986 The 3-D aspect of a turbulent plane wake flow. In *Proc. 3rd Asian Cong. of Fluid Mechanics, September 1–5, 1986, Tokyo* (ed. T. Matsui), pp. 206–209. Sato.

Hussain, A. K. M. F. 1981 Coherent structures and studies of perturbed and unperturbed jets. In *The Role of Coherent Structures in Modelling Turbulence and Mixing.* Lecture Notes in Physics, vol. 136 (ed. J. Jimenez), pp. 252–291. Springer.

Hussain, A. K. M. F. 1986 Coherent structures and turbulence. *J. Fluid Mech.* **173**, 303–356.

Jimenez, J., Cogollos, M. & Bernal, L. P. 1985 A perspective view of the plane mixing layer. *J. Fluid Mech.* **152**, 125–143.

Katz, K. & O'Hern, T. J. 1986 Cavitation in large scale shear flows. Trans. *ASME* I: *J. Fluids Engng* **108**, 373–376.

Kiya, M. & Matsumura, M. 1985 Turbulence structure in the intermediate wake of a circular cylinder. *Bull. JSME* **28**, 2617–2624.

† Another possibility is pairing instabilities. A way of distinguishing between two possibilities would be to educe structures containing two basic periods instead of just one. This was suggested by a referee and remains as a study for the future.

LASHERAS, J. C., CHO, J. S. & MAXWORTHY, T. 1986 On the origin and evolution of streamwise vortical structures in a plane, free shear layer. *J. Fluid Mech.* **172**, 231–258.

MEIBURG, E. & LASHERAS, J. C. 1987 Comparison between experiments and numerical simulations of three-dimensional plane wakes. *Phys. Fluids* **30**, 623–625.

PERRY, A. E. & STEINER, T. R. 1987 Large-scale vortex structures in turbulent wakes behind bluff bodies. Part 1. Vortex formation *J. Fluid Mech.* **174**, 233–270.

REYNOLDS, W. C. & HUSSAIN, A. K. M. F. 1972 The mechanism of an organized wave in turbulent shear flow. Part 3. Theoretical models and comparisons with experiments. *J. Fluid Mech.* **54**, 263–288.

STEINER, T. R. & PERRY, A. E. 19887 Large-scale vortex structures in turbulent wakes behind bluff bodies. Part 2. Far-wake structures. *J. Fluid Mech.* **174**, 271–298.

TANEDA, S. 1986 Irregular flows. In *Proc. 3rd Asian Cong. of Fluid Mech., September 1–5, 1986, Tokyo* (ed. T. Matsui), pp. 3–14. Sato.